Japanese Journal of Applied Physics

The Japan Society of Applied Physics

REGULAR PAPER

Fabrication of diamond/Cu direct bonding interface for power device applications

To cite this article: Shinji Kanda *et al* 2020 *Jpn. J. Appl. Phys.* **59** SBBB03

View the article online for updates and enhancements.

This content was downloaded from IP address 160.193.244.225 on 27/11/2019 at 01:45

Japanese Journal of Applied Physics 59, SBBB03 (2020)
https://doi.org/10.7567/1347-4065/ab4f19

REGULAR PAPER

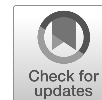

Fabrication of diamond/Cu direct bonding interface for power device applications

Shinji Kanda[1], Yasuo Shimizu[2], Yutaka Ohno[3], Kenji Shirasaki[2], Yasuyoshi Nagai[2], Makoto Kasu[4], Naoteru Shigekawa[1], and Jianbo Liang[1*]

[1]*Electronic Information Systems, Osaka City University, 3-3-138 Sumiyoshi, Osaka 558-8585, Japan*
[2]*Institute for Materials Research (IMR), Tohoku University, 2145-2 Narita, Oarai, Ibaraki 311-1313, Japan*
[3]*Institute for Materials Research (IMR), Tohoku University, 2-1-1 Katahira, Sendai 980-8577, Japan*
[4]*Department of Electrical and Electronic Engineering, Saga University, 1 Honjo-machi, Saga 840-8502, Japan*

[*]E-mail: liang@osaka-cu.ac.jp

Received August 7, 2019; revised September 11, 2019; accepted October 18, 2019; published online November 26, 2019

Direct bonding of diamond and Cu was successfully conducted by the surface activated bonding method at room temperature. The structure of the diamond/Cu bonding interface was investigated by transmission electron microscopy and electron energy-loss spectroscopy. The effect of heat treatment temperature on the interface structure was also investigated. A 4-nm-thick damaged layer was formed at the as-bonded interface, and the damaged layer's thickness decreased with an annealing temperature rise. It was found that the atomic ratio of sp^2 bonding in the bonding interface was larger than that of the diamond separated from the interface by approximately 50 nm, which indicates that the damaged layer was composed of amorphous carbon or graphite and diamond. After annealing at 700 °C, a composite layer about 2 nm thick was observed at the interface. There were no nano-voids or micro-cracks observed at the interface with annealing at a temperature as high as 700 °C. These results indicate that the diamond/Cu bonding interface has high thermal stability and can withstand the temperature rise of power devices during operation. © 2019 The Japan Society of Applied Physics

1. Introduction

Diamond has the highest thermal conductivity (22 W/cm · K) among materials and the most potential for suppressing the rise in device temperature when integrated with electronic devices. Diamond is being explored as an efficient heat spreader substrate for GaN-based devices.[1,2] AlGaN/GaN high-electron-mobility transistors (HEMTs) are commonly fabricated on SiC, sapphire, and Si substrates.[3–5] The thermal conductivities of SiC (4 W/cm · K), sapphire (0.5 W/cm · K), and Si (1.5 W/cm · K) are very low in comparison with that of diamond. The output power of AlGaN/GaN HEMTs is limited by the thermal conductivity of the substrate materials because the heat generated by self-heating mainly transfers through the substrate, which would degrade device performance and reliability.[6–8] It has been reported that AlGaN/GaN HEMTs grown on single-crystal diamond (111) substrates by metalorganic vapor-phase epitaxy obtain maximum drain current, cut-off frequency, and maximum oscillation frequency compared with those grown on SiC substrates.[9] The integration of GaN-based devices and diamond by direct growth and wafer bonding has been studied extensively in recent years, resulting in improved thermal management and a three-fold increase in the devices' output power.[10–12]

Diamond integrated with GaN-based devices needs to be directly mounted onto the heat sink by solder bonding or hydrophilic bonding for a device module.[13,14] The thermal conductivities of solder materials such as AgSn (0.33 W/cm · K) and AuSn (0.57 W/cm · K) are very low in comparison with those of heat sink materials like Al (2.36 W/cm · K) and Cu (3.98 W/cm · K). High thermal resistance would exist between the device and the heat sink, which would become a significant thermal barrier to heat transfer from the device to the heat sink.[15] Furthermore, solder bonding technology with an intermediate layer would significantly degrade the superiorities of the diamond used for the heat spreader substrate. Direct bonding of diamond and Al or Cu is the most promising method for heat transfer from the device to the heat sink. It has been reported that the direct bonding of diamond and Al is achieved at room temperature by surface activated bonding (SAB) and it obtains high thermal stability for the bonding interface.[16] Cu is superior to Al in terms of heat dissipation because the thermal conductivity of Cu is higher than that of Al. We previously succeeded in diamond and Cu direct bonding by SAB and obtained a bonding interface without nano-voids.[17] However, the structures of the bonding interface and the effects of the heating temperature on the bonding interface are still unknown, which are necessary to have a better understanding of the nature of the bonding interface for designing heat dissipation devices.

In this paper, we examine the structures of the diamond/Cu bonding interface and the effects of the heating temperature on the interfacial structure by transmission electron microscopy (TEM). The chemical bonding states of the bonding interface carbon atoms were investigated by electron energy-loss spectroscopy (EELS). The thermal stability of the bonding interface was tested at annealing temperatures as high as 700 °C in a N_2 gas atmosphere.

2. Experimental methods

A high-pressure, high-temperature synthesized single-crystal diamond substrate (100) and a Cu plate made by the rolling cylinder method were used for diamond/Cu direct bonding. The sizes of the diamond and Cu were 4 mm × 4 mm × 0.5 mm and 10 mm × 10 mm × 0.25 mm, respectively. The diamond surface was polished by mechanical polishing. The average roughness (Ra) of the polished diamond surface and Cu plate bonding surface was measured to be 0.32 nm and 30 nm by an atomic force microscope, respectively. First, the diamond and Cu were cleaned with acetone and isopropyl alcohol in an ultrasonic bath for 300 s, respectively, dried under N_2 flow, and then set in the chamber of a SAB facility. The surfaces of the diamond and Cu were activated by Ar fast atom beam irradiation in ultra-high vacuum conditions. After the surface activation, the diamond and Cu were brought into contact by applying a pressure of 10 MPa at room temperature; diamond/Cu direct bonding was achieved by SAB.[18–21] The structure of

 © 2019 The Japan Society of Applied Physics

the diamond/Cu bonding interface was investigated using TEM (JEM-2200FS) equipped with an EELS apparatus. Carbon K-shell edge spectra were measured between 225 and 375 eV at an accelerating voltage of 200 kV by EELS. The bonded samples were annealed separately at 500 and 700 °C for 5 min in ambient N_2 gas. The nano-structural behavior of the bonding interface after annealing was also investigated by TEM. The samples for TEM observation were fabricated using a focused ion beam (FIB) technique.

3. Results

An optical microscope image of the diamond/Cu bonded sample surface before annealing is shown in Fig. 1. The bonded area of the bonding interface is visible in the image because diamond is a transport material. Although a small unbonded region was observed on the upper left side of the bonded sample, an about 99% area bonding of the diamond and Cu was achieved. This result indicates that direct bonding of diamond and Cu could be formed at room temperature.

Figures 2(a)–2(c) show a cross-sectional TEM image of the as-bonded diamond/Cu interface, and the EELS spectra of the interface and the diamond separated from the interface by approximately 50 nm, respectively. A damaged layer was observed at the as-bonded interface; the damaged layer's thickness was estimated to be about 4 nm. No nano-voids or cracks were observed at the as-bonded interface, which indicates that an excellent bonding interface was obtained. Fitting of the EELS spectra was performed using a Gaussian function. As shown in Figs. 2(b) and 2(c), the EELS spectra of the as-bonded interface and diamond were decomposed into four peaks located at 284.2, 290.8, 296.7, and 305.3 eV, which were assigned to be π^*, σ_1^*, σ_2^*, and σ_3^* peaks, respectively. π^* and σ^* peaks are typical for indicative sp^2 hybridized carbon in graphite or amorphous carbon and tetrahedral coordination sp^3 carbon in diamond, respectively. By integrating the area of the decomposed peaks, the atomic ratio of sp^2 was given by[22]

$$sp^2(\%) = \frac{\pi^*/(\pi^* + \sigma^*)}{\pi^*_{graphite}/(\pi^*_{graphite} + \sigma^*_{graphite})} \quad (1)$$

where $\pi^*_{graphite}$ and $\sigma^*_{graphite}$ are the percentages of sp^2 and sp^3 bonding in a standard graphite carbon. Here, sp^2 bonding

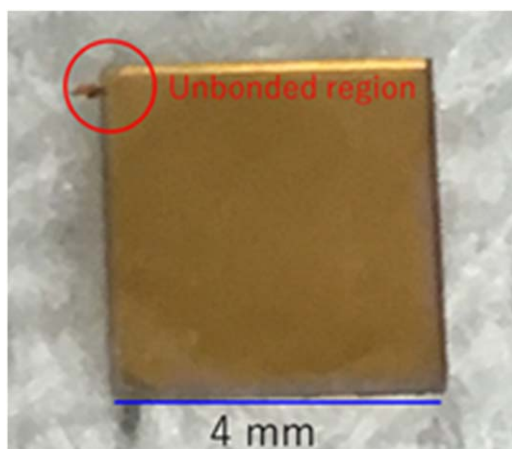

Fig. 1. (Color online) Optical microscope image of the diamond/Cu bonded sample surface without annealing.

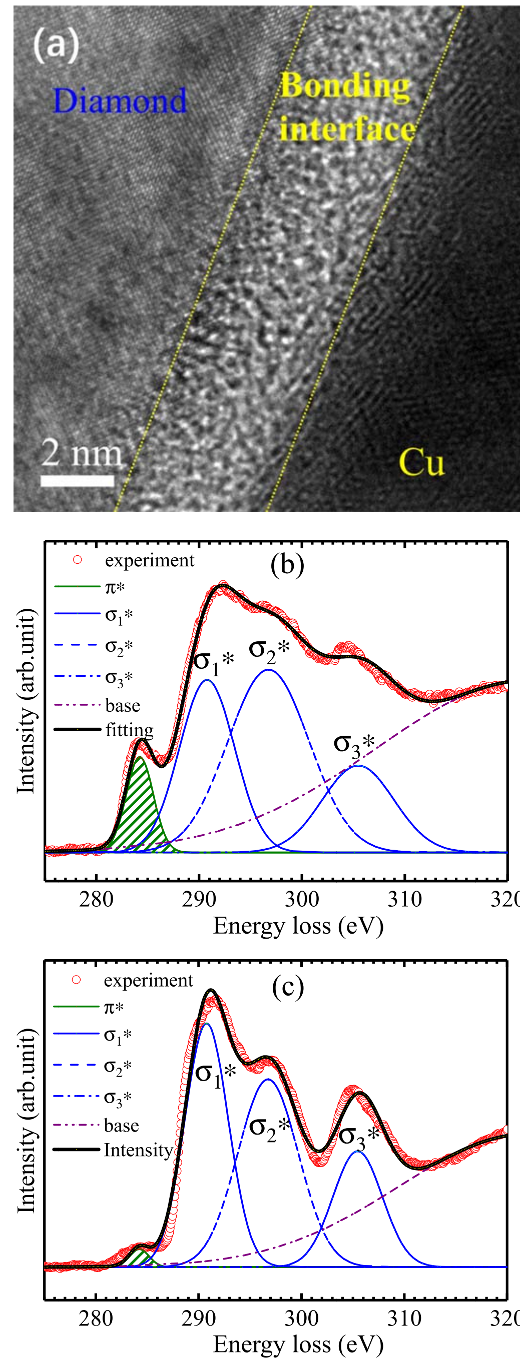

Fig. 2. (Color online) A cross-sectional TEM image of the as-bonded diamond/Cu interface (a), and EELS spectra of the interface (b) and the diamond separated from the interface by approximately 50 nm (c).

was assumed to be approximately 25%.[23–25] The atomic ratio of sp^2 bonding was calculated to be 28.3% and 3.6% in the interface and the diamond separated from the interface by approximately 50 nm, respectively.

Low-magnification cross-sectional TEM images of the as-bonded diamond/Cu interface and the interface annealed at 500 and 700 °C are shown in Figs. 3(a)–3(c), respectively. A straight line located in the center of the figures could be recognized, which corresponds to the interface of the diamond and Cu. Note that there are two holes observed in Fig. 3(c), which were induced by FIB irradiation during the TEM sample fabrication process. Lots of strain marks were observed on the Cu side of the as-bonded interface, which should have been caused in the Cu plate manufacturing

© 2019 The Japan Society of Applied Physics

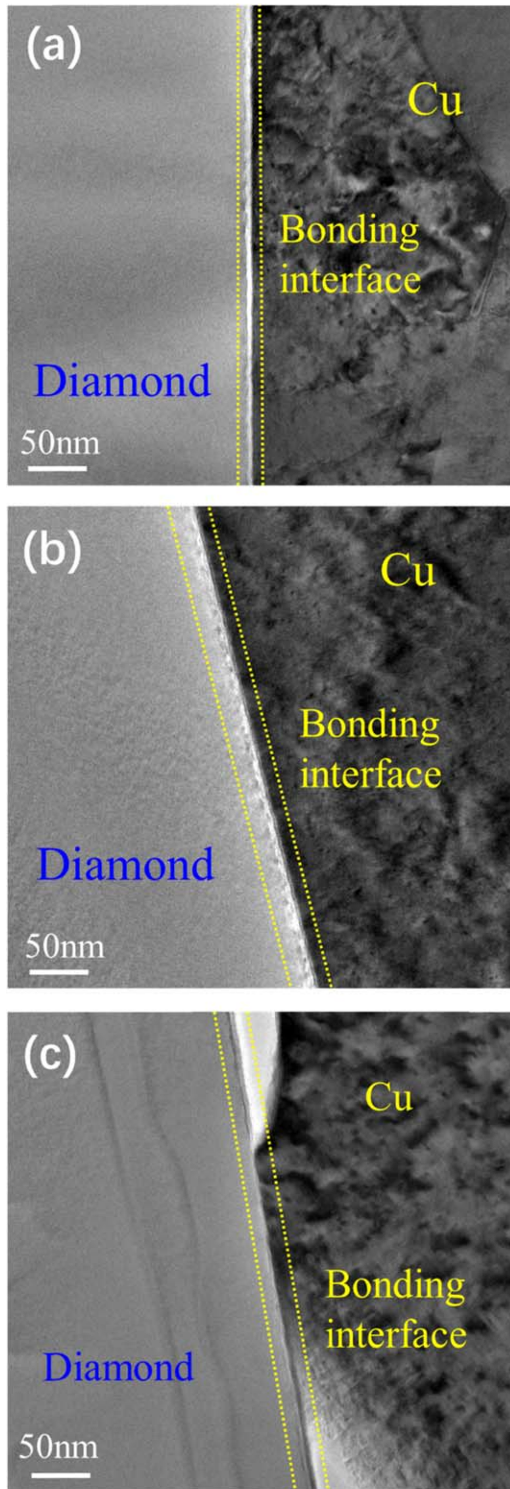

Fig. 3. (Color online) Low-magnification cross-sectional TEM images of the as-bonded diamond/Cu interface (a) and the interface annealed at 500 (b) and 700 °C (c).

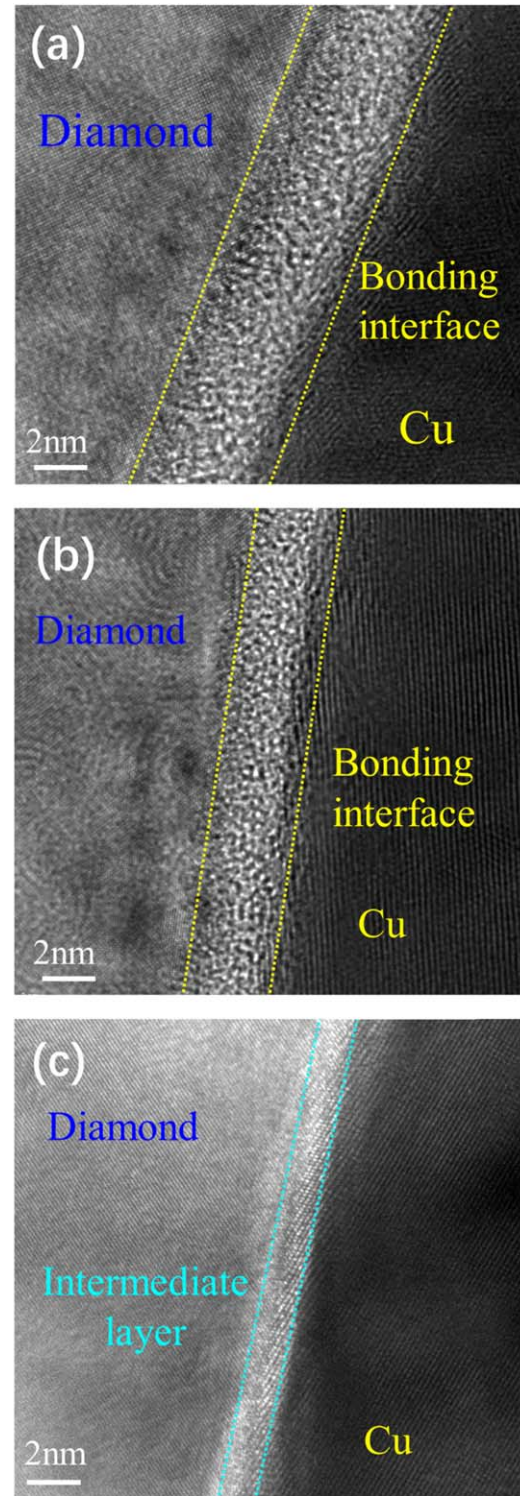

Fig. 4. (Color online) High-magnification cross-sectional TEM images of the as-bonded diamond/Cu interface (a) and the interface annealed at 500 (b) and 700 °C (c).

process by the roller compression. The load of 10 MPa applied to the bonding samples during the bonding process was unlikely to cause Cu strain. No cracks or micro-voids were observed near the as-bonded interface and the interface annealed at 500 °C. Even after annealing at a temperature as high as 700 °C, separation of the bonding interface was not observed.

Figures 4(a)–4(c) show high-magnification cross-sectional TEM images of the as-bonded diamond/Cu interface and the diamond/Cu interface annealed at 500 and 700 °C, respectively. A damaged layer with a thickness of about 4 nm was observed in the as-bonded interface. The damaged layer's thickness was decreased to 2.5 nm after annealing at 500 °C. After annealing at 700 °C, no damaged layer was observed at the interface. The damaged layer's thickness highly depended on the post-annealing temperature, which thinned with the annealing temperature. Instead of a damaged layer, a composite layer with a thickness of about 1 nm was formed

© 2019 The Japan Society of Applied Physics

at the interface. It is of paramount importance that there were no nano-cracks or voids observed at the interface as well as at the interface annealed at 700 °C. These results suggest that a diamond/Cu interface has high-temperature stability over a wide treatment temperature range.

4. Discussion

It was found that there was a damaged layer with a thickness of about 4 nm formed at the as-bonded interface [Fig. 2(a)]. Similar damaged layers have also been reported for Si/GaAs, GaAs/SiC, and Si/SiC bonding interfaces fabricated by SAB.[26–28] The damaged layer was formed due to Ar beam irradiation during the bonding process. The obtained atomic ratio value of sp^2 in the as-bonded interface was larger than that of the diamond separated from the interface by approximately 50 nm, which corresponds to the portion decrease of the diamond and the portion increase of the amorphous or graphite carbons. These resulted from the Ar beam irradiation process destroying the diamond crystal structure during the bonding process. It has been reported that the atomic ratio of sp^2 bonding is increased in polycrystal diamond by ion bombardment.[29] The observed small atomic ratio of sp^2 bonding in the diamond should be related to the FIB irradiation during the TEM sample fabrication process.

The damaged layer's thickness decreased with the annealing temperature increasing. Furthermore, no damaged layer was observed at the interface annealed at 700 °C. These results indicate that the post-annealing process had significant impact on the structural change of the damaged layer. According to our previous reports, the damaged layer disappears after annealing at high temperatures due to the recrystallization of the damaged layer.[28,30,31] For the diamond/Si bonding interface, a SiC intermediate layer was formed after annealing at 1000 °C, which played a role of residual stress relaxation between the diamond and Si.[31,32] Although the thermal expansion coefficient of Cu (16.42×10^{-6} K^{-1}) is much larger than that of diamond (2.3×10^{-6} K^{-1}),[33] no cracks or separation was observed at the diamond/Cu interface even after annealing at a temperature as high as 700 °C. These results should be related to the structural change of the damaged layer formed at the diamond/Cu interface.

The damaged layer consisted of Cu- and diamond-side damaged layers. The carbon atom of the diamond-side damaged layer diffused into the Cu-side damaged layer to form a composite layer of Cu and carbon after annealing at 700 °C. The thermal expansion coefficient of the composite layer should be larger than that of diamond and smaller than that of Cu. It has been reported that the thermal expansion coefficient of composite material composed of Cu and diamond decreases with an increasing diamond component.[34] The composite layer reduced the difference in thermal expansion coefficient between the Cu and diamond. The composite layer formed at the interface annealed at 700 °C served as a relaxation layer. The residual stress relaxation mechanism of the diamond/Cu bonding interface should be consistent with that of the diamond/Si bonding interface.[32] The crystal structure of the composite layer will be investigated in our next work.

It is true that the damaged layer's thickness was as thin as 4 nm, which hardly affected the thermal transfer across the bonding interface. Direct bonding of diamond and Cu is expected to reduce the thermal resistance between the device and heat sink. The minimum thermal resistance of the diamond/Cu bonding interface should be expected due to the absence of solder materials. Moreover, the diamond/Cu interface has high-temperature thermal stability at as high as 700 °C, which indicates that the bonding interface could withstand the high temperature generated during power device operation.

5. Conclusions

We investigated the structures of the bonding interface with annealing at various temperatures and demonstrated the thermal stability of the diamond/Cu bonding interface. A damaged layer was formed at the bonding interface, and its thickness decreased as the annealing temperature increased. Peaks corresponding to the π^* and σ^* orbitals were observed in the EELS spectrum of the interface and the amorphous or graphite carbon portion of the interface was larger than that of the diamond separated from the interface. After annealing at 700 °C, a composite layer was observed at the interface. No micro-cracks or nano-voids were observed at the interface with annealing at different temperatures. These results indicate that the diamond/Cu bonding interface has high thermal stability and could be useful for connecting diamond and heat sinks for high-power devices.

Acknowledgments

This study was supported partly by the Hirose International Scholarship Foundation and a Grant-in-Aid for Challenging Exploratory Research (18K19034) of the Ministry of Education, Culture, Sports, Science, and Technology, Japan. The fabrication of TEM samples by FIB and a part of TEM were, respectively, performed at The Oarai Center and at the Laboratory of Alpha-Ray Emitters in IMR under the Inter-University Cooperative Research Program in IMR (No. 18M0045 and 19M0037).

ORCID iDs

Yasuo Shimizu https://orcid.org/0000-0002-6844-8165

Yutaka Ohno https://orcid.org/0000-0003-3998-4409

Naoteru Shigekawa https://orcid.org/0000-0001-7454-8640

Jianbo Liang https://orcid.org/0000-0001-5320-6377

1) Y. Yamamoto, T. Imai, K. Tanabe, T. Tsuno, Y. Kumazawa, and N. Fujimori, Diam. Relat. Mater. **6**, 1057 (1997).
2) K. Nosaeva, N. Weimann, M. Rudolph, W. John, O. Krueger, and W. Heinrich, Electron. Lett. **51**, 1010 (2015).
3) Y.-F. Wu, D. Kapolnek, J. P. Ibbetson, P. Parikh, B. P. Keller, and U. K. Mishra, IEEE Trans. Electron Devices **48**, 2181 (2001).
4) V. Tilak, B. Green, V. Kaper, H. Kim, T. Prunty, J. Smart, J. Shealy, and L. Eastman, IEEE Electron Device Lett. **22**, 504 (2001).
5) Y.-F. Wu, A. Saxler, M. Moore, R. P. Smith, S. Sheppard, P. M. Chavarkar, T. Wisleder, U. K. Mishra, and P. Parikh, IEEE Electron Device Lett. **25**, 117 (2004).
6) G. Meneghesso, G. Verzellesi, F. Danesin, F. Rampazzo, F. Zanon, A. Tazzoli, M. Meneghini, and E. Zanoni, IEEE Trans. Device Mater. Reliab. **8**, 332 (2008).
7) R. Gaska, A. Osinsky, J. Yang, and M. S. Shur, IEEE Electron Device Lett. **19**, 89 (1998).
8) A. Sarua, H. Ji, M. Kuball, M. J. Uren, T. Martin, K. P. Hilton, and R. S. Balmer, IEEE Trans. Electron Devices **53**, 2438 (2006).

© 2019 The Japan Society of Applied Physics

9) K. Hirama, Y. Taniyasu, and M. Kasu, Appl. Phys. Lett. **98**, 162112 (2011).
10) H. Sun, R. B. Simon, J. W. Pomeroy, D. Francis, F. Faili, D. J. Twitchen, and M. Kuball, Appl. Phys. Lett. **106**, 111906 (2015).
11) D. Francis, F. Faili, D. Babic, F. Ejeckam, A. Nurmikko, and H. Maris, Diam. Relat. Mater. **19**, 1525 (2012).
12) J. W. Pomeroy, M. Bernardoni, D. C. Dumka, D. M. Fanning, and M. Kuball, Appl. Phys. Lett. **104**, 083513 (2014).
13) M. Kuznetsov, F. Hakimi, R. Sprague, and A. Mooradian, IEEE Photonics Technol. Lett. **9**, 1063 (1997).
14) Z. L. Liau, Appl. Phys. Lett. **77**, 651 (2000).
15) A. Saura, H. Ji, K. P. Hilton, D. J. Wallis, M. J. Uren, T. Martin, and M. Kuball, IEEE Trans. Electron Devices **54**, 3152 (2007).
16) J. Liang, S. Yamajo, M. Kuball, and N. Shigekawa, Scr. Mater. **159**, 58 (2019).
17) S. Kanda, S. Masuya, M. Kasu, N. Shigekawa, and J. Liang, Proc. 6th Int. IEEE Workshop Low-Temperature Bonding for 3D Integration, 2019, p. 57.
18) H. Takagi, K. Kikuchi, R. Maeda, T. R. Chung, and T. Suga, Appl. Phys. Lett. **68**, 2222 (1996).
19) J. Liang, T. Miyazaki, M. Morimoto, S. Nishida, and N. Shigekawa, J. Appl. Phys. **114**, 183703 (2013).
20) T. H. Kim, M. M. R. Howlader, T. Itoh, and T. Suga, J. Vac. Sci. Technol. **21**, 449 (2003).
21) J. Liang, S. Masuya, M. Kasu, and N. Shigekawa, Appl. Phys. Lett. **110**, 111603 (2017).
22) P. J. Fallon and L. M. Brown, Diam. Relat. Mater. **2**, 1004 (1993).
23) D. F. R. Mildner and J. M. Carpenter, J. Non-Cryst. Solids **47**, 391 (1982).
24) C. Gao, Y. Y. Wand, A. L. Ritter, and J. R. Dennision, Phys. Rev. Lett. **62**, 954 (1989).
25) G. Galli, R. M. Martin, R. Car, and M. Parrinello, Phys. Rev. Lett. **62**, 555 (1989).
26) J. Liang, T. Miyazaki, M. Morimoto, S. Nishida, N. Watanabe, and N. Shigekawa, Appl. Phys. Express **6**, 021801 (2013).
27) E. Higurashi, K. Okumura, K. Nakasuji, and T. Suga, Jpn. J. Appl. Phys. **54**, 030207 (2015).
28) J. Liang, S. Nishida, M. Arai, and N. Shigekawa, Appl. Phys. Lett. **104**, 161604 (2014).
29) D. Bullutaud, N. Simon, H. Girard, E. Rzepka, and B. Bouchet-Fabre, Diam. Relat. Mater. **15**, 716 (2006).
30) S. Yamajo, S. Yoon, J. Liang, H. Sodabanlu, K. Watanabe, M. Sugiyama, A. Yasui, E. Ikenaga, and N. Shigekawa, Appl. Surf. Sci. **473**, 627 (2019).
31) J. Liang, S. Masuya, S. Kim, T. Oishi, M. Kasu, and N. Shigekawa, Appl. Phys. Express **12**, 016501 (2019).
32) J. Liang, Y. Zhou, S. Masuya, F. Gucmann, M. Singh, J. Pomeroy, S. Kim, M. Kuball, M. Kasu, and N. Shigekawa, Diam. Relat. Mater. **93**, 187 (2019).
33) K. Yoshida and H. Morigami, Microelectron. Reliab. **44**, 303 (2004).
34) T. Guillemet, P. M. Geffroy, J. M. Heintz, N. Chandra, Y. F. Lu, and J. F. Silvain, Composites A **43**, 1746 (2012).

© 2019 The Japan Society of Applied Physics